

# Influence of TEMPO-oxidized cellulose nanofibrils on the properties of filler-containing papers

Ana F. Lourenço<sup>a</sup>, José A.F. Gamelas<sup>a</sup>, Tiago Nunes<sup>a</sup>, José Amaral<sup>b</sup>, Peré Mutjé<sup>c</sup>, Paulo J. Ferreira<sup>a,\*</sup>

<sup>a</sup> CIEPQPF, Department of Chemical Engineering, University of Coimbra, Pólo II. R. Sílvio Lima, PT - 3030-790 Coimbra, Portugal

<sup>b</sup> RAIZ – Forest and Paper Research Institute, Quinta de São Francisco, Apartado 15, PT - 3801-501 Eixo, Portugal

<sup>c</sup> Department of Chemical Engineering, LEPAMAP, University of Girona, c/M. Aurèlia Campmany, no. 61, Girona 17071, Spain

\*[paulo@eq.uc.pt](mailto:paulo@eq.uc.pt); Tel: 00351239798747; fax: 00351239798703

## Abstract

In this work, cellulose nanofibrils (CNF) were produced from a *Eucalyptus globulus* bleached kraft pulp by TEMPO-mediated oxidation and mechanical homogenization, and their effect in papermaking, namely filler flocculation and retention, dry and wet-web strength and structural properties, was studied in detail.

Cellulose nanofibrils possessing 0.6 mmol/g of carboxyl groups and a degree of polymerization (DP) of *ca.* 550 were found to promote filler flocculation and retention in the fibre mat whereas the same amount (3 wt%) of CNF having 1.5 mmol/g of carboxyl groups, a DP of *ca.* 200 and a similar mean diameter, exhibited an opposite effect. These results were interpreted with the help of flocculation studies of precipitated calcium carbonate (PCC) in the presence of CNF carried out by laser diffraction spectrometry. In addition, the mechanical and structural properties of the handsheets were analyzed revealing that the less charged CNF led to more closed matrices and, even increasing the filler retention, had a positive role on the tensile strength. A bonding mechanism between eucalypt fibres, PCC, CNF and a linear cationic polyacrylamide is proposed, consistent with the flocculation, retention and paper strength and structural properties results. It is concluded that, to be used in papermaking, the CNF must not have a high charge (nor a small length) in order to be able to flocculate the filler particles and, at the same time, to increase the filler-to-cellulosic fibres bonding.

A complementary study on the wet-web resistance of handsheets produced with the less charged CNF was conducted for moisture contents between 10 and 70% showing that this CNF can significantly improve the handsheets wet tensile strength (nearly 100%) even for water contents above 50%. The use of CNF in the paper machine may thus contribute, through the higher wet-web tensile resistance, to reduce breaks and increase the operating speeds and, through the higher filler retention, to important fibre and cost savings.

## 43 **Keywords**

44 *Cellulose nanofibrils; Flocculation; Papermaking; Filler retention; Tensile*  
45 *strength*

46

## 47 **Introduction**

48 Cellulose nanofibrils (CNF) are a promising and interesting material for different  
49 industrial applications as widely reported in the literature. They comprise fibrils  
50 with a high aspect ratio having diameters of less than 50 nm and lengths of a few  
51 micrometres, and can be obtained from wood or non-woody resources by using,  
52 preferentially, chemical (e.g. TEMPO-mediated or periodate-chlorite oxidations  
53 or carboxymethylation) or enzymatic pre-treatments, followed by mechanical  
54 treatments (e.g., homogenization, grinding, ultra-sonication). If only mechanical  
55 energy is used significantly lower amounts of nano-sized material are obtained.  
56 CNF possess very high stiffness (Young's modulus higher than 10 GPa) (Kangas  
57 et al. 2014) and high specific surface area (about ten times greater than that of the  
58 original fibers) (Lavoine et al. 2012), which make them highly suitable to be used  
59 as mechanical reinforcement material of diverse matrices (Eichorn et al. 2010;  
60 Khalil et al. 2014). For instance, they can enhance the strength properties of a  
61 cellulose matrix by promoting a better bonding between the cellulosic fibres  
62 (Taipale et al. 2010; González et al. 2014). In papermaking, they have also the  
63 potential to be used in a) paper coating, either to improve the barrier properties  
64 and/or the printing quality, b) as flocculant of mineral fillers or c) as rheology  
65 control additive (Klemm et al. 2011; Brodin et al. 2014). However, the research  
66 in the papermaking field is still mainly focused in the production and uses of the  
67 so-called "nanopapers" since CNF fibres have strength and gas barrier properties  
68 that make them suitable to be used as substrate for diverse applications such as in  
69 food packaging or printed electronics devices (Syverud and Stenius 2009;  
70 Henriksson et al. 2008; Fukuzumi et al 2009; Chinga-Carrasco et al. 2012;  
71 Lavoine et al. 2012; Torvinen et al. 2012; González et al. 2014).

72 The increase of the tensile index in lab handsheets, having only fibres and  
73 CNF, has been reported by several authors that claim that extensive hydrogen  
74 bonds are formed. Ioelovich and Figovsky (2010) found that the introduction of  
75 cellulose nanofibres increased significantly the handsheets strength while the  
76 porosity was decreased. In the same way, González et al. (2012) stated that by

77 incorporating 6 to 9% (w/w) of CNF in an unbeaten bleached *Eucalyptus* pulp  
78 furnish, the strength properties were similar to those of handsheets produced only  
79 with the corresponding refined pulp (23 °SR). Petroudy et al. (2014) explored the  
80 benefits of using a cationic polyacrylamide together with CNF to produce stronger  
81 handsheets without disturbing the porosity. The main drawback in all these studies  
82 was the decrease of drainability during sheet formation. However, Taipale et al.  
83 (2010) concluded that by the optimum selection of the materials and process  
84 conditions, the strength of paper can be improved without significantly affecting  
85 drainability.

86 The aforementioned bonding potential of the CNF is related to the high  
87 specific surface area and –OH groups available for hydrogen bonds. Besides, for  
88 the TEMPO-oxidized CNF (TOCN), it has been proposed by Saito and Isogai  
89 (2006, 2007) that the aldehyde groups derived from the oxidation at the surface of  
90 the cellulose fibres contribute to the wet strength development of the fibrous  
91 matrix because covalent bonds are formed through hemiacetal linkages between  
92 the hydroxyl and the aldehyde groups. Noteworthy that in all the studies  
93 previously referred to, no mineral fillers were used.

94 As well known, fillers are used to improve several paper properties (e.g., light  
95 scattering coefficient, opacity, surface smoothness) besides being cheaper than  
96 fibres, but they aggregate between fibres and prevent fibre-to-fibre bonds, thus  
97 causing a loss of paper strength (Raymond et al. 2004; Hubbe 2014). Therefore,  
98 the filler content in paper is limited to amounts rarely superior to 30%.

99 The interaction of CNF with mineral fillers, during the sheet formation, has been  
100 evaluated in a small number of studies and is not yet completely understood given  
101 the diversity of variables involved, namely e.g. the nature of fillers and  
102 nanofibrils. Ämmälä et al (2013) showed that the addition of TEMPO-oxidized  
103 and periodate-chlorite oxidized CNF to a furnish containing fibres and ground  
104 calcium carbonate (GCC) increased significantly the filler retention (from about  
105 50-55% to 85-95%). Since GCC and oxidised CNF were all negatively charged, a  
106 patching flocculation mechanism involving  $\text{Ca}^{2+}$  ions from dissociated GCC was  
107 proposed. However, both types of CNF seemed not to have any positive effect on  
108 the handsheets tensile strength, and this was attributed to poor sheet formation. In  
109 another study, Hii et al. (2012) studied the interactions between fillers, CMF (not  
110 chemically pre-treated cellulose microfibrils) and fibres after wet pressing. Since

111 CMF possess a strong water retention capability which disturbs dewatering (as  
112 well as CNF), the authors used high contents of filler aiming at obtaining a better  
113 pressability. The conclusion was that by adequately selecting the CMF and the  
114 filler content it was possible to improve the strength properties without affecting  
115 the pressability of the sheet in the wet-end. Besides, the filler together with CMF  
116 also led to an increase of the handsheets light scattering and air resistance because  
117 the CMF proved to effectively bind the fillers in the fibre network. Quite recently,  
118 He et al. (2016) reported that a composite of CMF, PCC and cationic starch  
119 provided handsheets of bleached kraft pulp (BKP) fibres with better strength  
120 properties and denser sheets. The CMF were obtained only by mechanical  
121 treatment of hardwood BKP fibres.

122 Korhonen and Laine (2014) studied the flocculation and retention mechanisms  
123 of fillers in the presence of CNF, concluding that TEMPO-CNF and  
124 carboxymethylated CNF can be used as effective precipitated calcium carbonate  
125 (PCC) flocculants, acting by a hybrid mechanism of bridging and patching.  
126 Interestingly, chemically unmodified CMF had no flocculation ability. Thus, the  
127 authors stated that CNF must have a high number of charged groups in order to  
128 increase their electrostatic interactions with the other components of the paper  
129 matrix. Nonetheless, they did not evaluate the standard properties of paper sheets  
130 containing CNF and PCC. It must be stressed that, in spite of the different studies  
131 mentioned above, the combined effect of fibres, fillers, CNF, retention and sizing  
132 agents, supported on flocculation studies and including also the evaluation of the  
133 wet-web strength, has not yet been reported in the literature.

134 In this context, the objective of the present work was (a) to evaluate the filler  
135 retention and the main structural and mechanical properties of dry handsheets  
136 prepared with fibres, small amounts of TEMPO-oxidized CNF (with different  
137 carboxyl groups content and size), mineral filler (PCC), and a cationic  
138 polyacrylamide (commonly used as retention agent), (b) to study the influence of  
139 the CNF on the flocculation of the filler particles, (c) to suggest a mechanism for  
140 the interactions between the different components of the furnish when CNF and  
141 CPAM are used and, (d) to study the influence of CNF on the wet-web resistance  
142 of handsheets containing filler (by testing specimens with different moisture  
143 contents).

144

## 145 **Materials and methods**

### 146 **CNF preparation and characterization**

147 To produce the TEMPO-oxidized CNF, a bleached *Eucalyptus globulus* kraft pulp  
148 was pre-treated with NaClO and catalytic amounts of TEMPO (2,2,6,6-  
149 tetramethylpiperidine-1-oxyl radical) and NaBr according to a methodology  
150 described elsewhere (Saito et al. 2007). The cellulose fibres were previously  
151 refined at 4000 rev. in a PFI beater before chemical oxidation. Briefly, 30 g (dry  
152 basis) of refined fibres were dispersed in distilled water containing TEMPO  
153 (0.016 g per g of fibres) and NaBr (0.1 g per g of fibres) at a consistency of 1%.  
154 The mixture was stirred for 15 min at room temperature in order to assure a good  
155 dispersion of all the components. Then, a NaClO solution (12.5% active chlorine)  
156 was slowly added to the previous mixture. Two samples were produced using 5  
157 and 11 mmol of NaClO per gram of cellulose, herein noted as CNF5 and CNF11,  
158 respectively. The pH of the medium was kept at 10 by the addition of drops of  
159 NaOH 0.1 M. The reaction was considered finished when the pH stabilized at 10  
160 (after 2 hours). The oxidised fibres were then filtered and washed with distilled  
161 water until the filtrate conductivity reached low values (*ca.* 10  $\mu$ S/cm). The fibres  
162 were then mechanically treated by high pressure homogenization: the fibres  
163 passed 5 times at 300 bar and 5 times at 600 bar (GEA Niro Soavi Panda Plus  
164 2000, Italy).

165

166 To evaluate the “yield” of the production of nanofibrillar material, 40 mL of  
167 the dispersions (0.2 wt%) were centrifuged at 9000 rpm for 30 min: the  
168 percentage (w/w) of supernatant material was considered the yield of fibrillation  
169 (Saito and Isogai 2006; Saito et al. 2009). The results were determined in  
170 duplicate.

171 The nanofibrils were then characterized for the cationic demand, carboxyl  
172 groups content, degree of polymerization, specific surface area and size. The  
173 cationic demand (CD) was measured in a Mütek PCD 04 particle charge detector,  
174 by using poly-DADMAC and Pes-Na cationic and anionic titrants, respectively,  
175 according to the methodology followed by Espinosa et al. (2016). The volume of

176 anionic polymer consumed until the equipment registered 0 mV was used to  
177 calculate the cationic demand according to eq.1

$$178 \quad CD = [(C_{PDADMAC} \cdot V_{PDADMAC}) - (C_{PESNA} \cdot V_{PESNA})]/m \quad (1)$$

179 where,

180 CD – Cationic demand ( $\mu\text{eq/L}$ )

181  $C_{PDADMAC}$  - Cationic polymer concentration (g/L)

182  $C_{PESNA}$  – Anionic polymer concentration (g/L)

183  $V_{PDADMAC}$  – Volume used of cationic polymer (L)

184  $V_{PESNA}$  – Volume used of anionic polymer (L)

185 m - Mass of CNF on dry basis (g)

186

187 The carboxyl's content ( $C_{COOH}$ ) was determined in triplicate by  
188 conductometric titration of aqueous suspensions of CNF (acidified to pH of ca. 3)  
189 with NaOH 0.01 M. The carboxyl's content was determined from the conductivity  
190 curve according to eq.2 (Kekäläinen et al. 2014).

$$191 \quad C_{COOH} = (V_2 - V_1)/m \cdot [NaOH] \quad (2)$$

192 where,

193  $C_{COOH}$  - Carboxyl groups content on dry basis of CNF (mmol/g)

194  $V_2 - V_1$  - Volume of NaOH solution added between the equivalence points (mL)

195 m - Mass of CNF on dry basis (g)

196  $[NaOH]$  - NaOH concentration (mmol/mL)

197

198 The degree of substitution (DS) of carboxyl groups of the CNF was estimated  
199 from the CNF carboxyl's content, following eq. 3.

$$200 \quad DS = C_{COOH} / [C_{COOH} + (1 - C_{COOH} \cdot 198.1) / 162.1] \quad (3)$$

201 where C is the CNF carboxyl's content (mol/g), 162.1 and 198.1 are the molar  
202 masses (g/mol) of the anhydroglucose units and of units substituted at C-6  
203 position by  $\text{COO}^- \text{Na}^+$  groups, respectively.

204

205 The degree of polymerization (DP) was determined from intrinsic viscosity  
206 measurements by dissolving the CNF samples in cupriethylenediamine (ISO  
207 5351:2010). The Mark Houwink equation (eq. 3) was applied for the calculations.

$$208 \quad [\eta] = K \cdot DP^a \quad (3)$$

209 where,

210  $\eta$  – intrinsic viscosity  
211  $K, a$  – Mark Houwink parameters:  $K=2.28, a=0.76$  (Henriksson et al. 2008)  
212 DP – Degree of polymerization

213

214 AFM images were used to assess the nanofibrils diameter. AFM imaging was  
215 performed on a film prepared by solvent casting of CNF5 in an AFM microscope  
216 from Bruker Innova using the peak force tapping mode, at room temperature, in  
217 air, with a silicon cantilever with a tip with a radius of 8 nm. The size of the  
218 assessed areas was  $2 \mu\text{m} \times 2 \mu\text{m}$ . However, as well known, the results obtained,  
219 besides being operator dependent, are restricted to the analysis of a small amount  
220 of sample and therefore the corresponding mean diameter is not representative of  
221 all the material. For this reason, a mean diameter was theoretically calculated  
222 assuming a cylindrical geometry and based on the specific surface area of the  
223 nanofibrils (SSA), as reported in the literature (Espinosa et al., 2016):

$$224 \quad d=4/(SSA \times \rho) \quad (4)$$

225 where,

226  $d$  – CNF diameter (nm)

227 SSA – CNF specific surface area ( $\text{m}^2/\text{g}$ )

228  $\rho$  - cellulose density =  $1,6 \text{ g/cm}^3$

229

230 The specific surface area (SSA) of the nanofibrils was theoretically calculated  
231 from the specific surface area of a single poly-DADMAC molecule ( $SSA_{\text{DADMAC}}$ )  
232 according to equation (5) explained in detail elsewhere (Espinosa et al., 2016).

$$233 \quad SSA = (CD - C_{\text{COOH}}) \times SSA_{\text{DADMAC}} \quad (5)$$

234

235 Dynamic light scattering (DLS) measurements were made in triplicate on the  
236 supernatants obtained after centrifugation of the CNF dispersions using a  
237 Zetasizer Nano ZS (Malvern Instruments), in order to have an idea of the relative  
238 size of the fibrils, as previously reported (Gamelas et al. 2015a).

239 FTIR-ATR spectra of CNF films were obtained on a Bruker Tensor 27  
240 spectrometer using a MKII Golden Gate accessory with a diamond crystal  $45^\circ$  top  
241 plate. The spectra were recorded in the  $500\text{--}4000 \text{ cm}^{-1}$  range with a resolution of  
242  $4 \text{ cm}^{-1}$  and a number of scans of 256.

243

## 244 **Handsheets preparation and characterization**

245 Before producing the handsheets the different paper components were prepared.  
246 *Eucalyptus globulus* bleached kraft pulp (34 °SR) was used as the cellulosic fibre  
247 source for the handsheets production. After disintegration the pulp was diluted to  
248 a consistency of 1% in demineralized water. Aqueous suspensions (0.2 wt%) of  
249 each CNF were magnetically stirred for 1 hour. PCC with a median diameter ( $d_{50}$ )  
250 of the particle size distribution (as measured by laser diffraction spectrometry) of  
251 4.4  $\mu\text{m}$  and a zeta potential of +7 mV was used as filler in the handsheets  
252 production. Aqueous suspensions of PCC (1 wt%) were stirred magnetically (20  
253 min) and sonicated (15 min, 50 KHz). A 3% starch suspension standing at 60 °C  
254 was also prepared according to a procedure detailed elsewhere (Saraiva et al.  
255 2010). Alkenyl succinic anhydride (ASA) was used as internal sizing agent and it  
256 was added to the starch suspension before mixture with the other components of  
257 the furnish. A 0.025% aqueous solution of a linear cationic polyacrylamide (C-  
258 PAM, commercial Percol 47, from BASF), with a high molecular weight and a  
259 low charge density, was used as retention agent. All the aforementioned additives  
260 were supplied by the industry.

261 According to the literature several routes may be adopted regarding the  
262 sequence of addition of the components when preparing the handsheets (Brodin et  
263 al. 2014). The most common are a) CNF addition to the mineral charges and  
264 thereafter the addition of the resultant mixture to the fiber suspension (Ämmälä et  
265 al. 2013; He et al. 2016), b) addition of all the components at once (Hii et al.  
266 2012) or c) addition of CNF to a mixture of fibre and filler (Korhonen and Laine  
267 2014). In the present work, preliminary studies showed that the mechanical  
268 properties of the handsheets, as well as the filler retention, had a bigger  
269 improvement by using the first strategy. Thus, PCC suspensions were mixed with  
270 the CNF dispersions at a PCC:CNF ratio of 10:1 (w/w) prior to the addition to the  
271 fibres suspension.

272 Handsheets were produced in a batch laboratory sheet former (255/SA model,  
273 MAVIS) using a 120 mesh screen. The aim was to achieve a basis weight of  
274 80g/m<sup>2</sup>. Amounts of 30, 3, 1, 0.12 and 0.02 wt% for PCC, CNF, starch, ASA and  
275 C-PAM, respectively, were used. For the handsheets production, the filler  
276 suspension (containing CNF/PCC or only PCC for comparison) was added to the  
277 fibre suspension. After 120 s of stirring, the starch/ASA mixture (at ca. 60 °C)



278 was added. C-PAM was then added after a total time of 290 s and allowed to stir  
279 for more 5 s. The mixture was transferred into the sheet former and after 10 s of  
280 air agitation drainage was performed. The drainage time was measured.

281 In a first series of experiments, the sheets were collected from the web and  
282 pressed, dried, and conditioned according to the ISO 5269-1 standard. The  
283 structural properties (basis weight, thickness, bulk, and air permeability) were  
284 measured according to the corresponding ISO Standard Test Methods. Besides,  
285 the handsheets porosity was analyzed by Hg intrusion porosimetry in an AutoPore  
286 IV 9500 instrument from Micromeritics and a surface analysis was performed by  
287 field-emission scanning electron microscopy (FE-SEM) in a Carl Zeiss Merlin  
288 microscope, in secondary electron mode, without any further coating.

289 For the wet-web resistance tests, a rectangular metallic mold was coupled to  
290 the sheet former screen in order to form test specimens that were collected from  
291 the web and pressed. In this case, different pressure levels were used in order to  
292 obtain specimens with different moisture contents, which, next, were tested in a  
293 vertical tensile test machine with a cell load of 50 N. The handsheets were  
294 weighed before and after drying (for five hours at 105 °C) which allowed to obtain  
295 the corresponding water content.

296 In both experiments the handsheets were calcined at 525 °C for 16 h to  
297 determine the PCC effective content (and the corresponding filler retention),  
298 according to the TAPPI Standard T211 om-93.

299

### 300 **Flocculation studies of PCC in the presence of CNF**

301 To better understand the interaction between CNF and PCC and the filler  
302 retention mechanism, the flocculation of the mineral particles in the presence of  
303 CNF was studied by measuring the evolution of the aggregates size with time, by  
304 laser diffraction spectrometry (LDS) in a Mastersizer 2000 equipment (Malvern  
305 Instruments). Previously to the measurements, a 1 wt% aqueous suspension of  
306 PCC and a 0.2 wt% aqueous suspension of each of the CNF samples were  
307 prepared as described before for the handsheets production. For the flocculation  
308 studies a 10:1 PCC:CNF ratio was used, also similarly to the handsheets  
309 preparation. For that, 9 mL of the PCC suspension were added to the equipment  
310 vessel containing 700 mL of distilled water (total solids concentration around 0.01  
311 wt%), and the tests were carried out by setting the pump speed at 2000 rpm. After

312 10 min. of agitation, 4.5 mL of the 0.2 wt% CNF suspension was added and 20  
313 min. later sonication was applied during 15 min. The measurement was continued  
314 until the agglomerates size stabilized (*ca.* 90 min. total). Tests with only PCC  
315 were also performed for comparison. The results presented are a mean of two  
316 measurements, for the three series of experiments: PCC, PCC+CNF5 and  
317 PCC+CNF11.

318

## 319 **Results and Discussion**

### 320 **CNF characterization**

321 Cellulose nanofibrils with two different contents of carboxyl groups were  
322 produced by NaClO oxidation mediated by TEMPO as mentioned above. Their  
323 main characterization data are listed in Table 1. The nanofibres production yield  
324 was very high for both CNF samples and in agreement with values expected for  
325 TEMPO-oxidized CNF (Besbes et al. 2011; Isogai et al. 2011). The nanofibres  
326 production yield was smaller for the sample with milder chemical treatment  
327 (CNF5) confirming that bigger fibres were still present. These results were in  
328 accordance with the degree of polymerization determined for both samples: CNF5  
329 with a higher DP than CNF11.

330

331

Insert Table 1

332

333 By doubling the amount of NaClO in the TEMPO-mediated oxidation, the  
334 cationic demand of CNF becomes much higher than that obtained for CNF5, as  
335 expected. Accordingly, the determination of the carboxyl group's content showed  
336 that CNF11 possessed more than the double of the carboxyl's of CNF5.  
337 Consequently, a degree of substitution of 0.10 and 0.26 was obtained for CNF5  
338 and CNF11, respectively (Table 1). A similar increase of carboxyl's content with  
339 the amount of NaClO used in the oxidation reaction has been previously reported  
340 (Saito and Isogai 2004; Isogai et al. 2011). Besides, the carboxylate surface  
341 density, obtained by the ratio between the carboxyl content measured for each  
342 sample and the corresponding specific surface area calculated values, is also much  
343 higher for the CNF11 nanofibrils: 5.1 mmol/m<sup>2</sup> vs. 3.5 mmol/m<sup>2</sup> for CNF5.  
344 Additionally, the different carboxyl's content of the two CNF was assessed by

345 FTIR-ATR spectroscopy. A high intensity band at  $1601\text{ cm}^{-1}$  due to the  
346 asymmetric COO stretching of the ionized  $\text{COO}^-$  groups was evident in the  
347 spectrum of CNF11, while for CNF5 this band was of much lower relative  
348 intensity (Fig. 1), confirming that the latter presented a considerably lower  
349 amount of carboxyl groups (Gamelas et al. 2015b).

350

351

Insert Fig. 1

352

353 The yield values, cationic demand and carboxyl groups were in agreement  
354 with the expected smaller size of the CNF11 nanofibrils. This fact was confirmed  
355 by comparing the fibrils size (Z-average) of both samples, as evaluated by DLS. It  
356 should be emphasized that DLS alone cannot be used to compute the size of the  
357 nanofibrils due to their acicular shape, but even though, it provides important and  
358 meaningful information regarding the size comparison of samples with similar  
359 structure, besides measuring a significant amount of fibrils (Gamelas et al. 2015a).

360 The CNF AFM image (Fig. 2a) reveals the great heterogeneity of the  
361 nanofibres size, as usual for this type of material (Besbes et al. 2011, Hänninen et  
362 al. 2015). This was confirmed by the diameter distributions plotted in Fig. 2b:  
363 values between 5 and 40 nm can be found.

364

365

Insert new Figure 2

366

367 Considering this broad range and the aforementioned limited  
368 representativity of any average value based on AFM imaging, it was decided to  
369 calculate a mean diameter using parameters representative of the whole samples –  
370 the cationic demand and the carboxyl group's content, as already supported in the  
371 literature (Espinosa et al., 2016). Values of 14.7 nm and 8.7 nm, respectively for  
372 CNF5 and CNF11, were obtained. However, it is legitimate to conclude that these  
373 differences are not significant taking into account the above referred to diversity  
374 of the nanofibrils diameter detected by AFM. Thus, based on the different degree  
375 of polymerization values, it may be concluded that both samples differ in the  
376 fibrils length rather than in the fibrils diameter. This difference was supported by  
377 the DLS Z-average values (used only for comparison purposes). Thus, the CNF

378 influence on filler flocculation and on the papermaking properties will be  
379 discussed based on the different carboxyl groups content and on the length.

380

### 381 **Flocculation studies of PCC in the presence of CNF**

382 Additional insight into the processes of PCC retention in the presence of CNF  
383 was obtained using laser diffraction spectrometry. The results of the evolution of  
384 the median ( $d_{50}$ ) of the particle size distribution with time for suspensions of PCC  
385 with and without CNF are shown in Fig. 3. When measuring only PCC, the  $d_{50}$   
386 increased slowly along the experiment, even with sonication, up to *ca.* 9  $\mu\text{m}$  after  
387 80 min, which is a common behavior for this material (Rasteiro et al. 2008). With  
388 the addition of the nanofibrils with lower carboxyl's content (and carboxyl's  
389 surface density, CNF5) to the PCC suspension, the  $d_{50}$  increased from 4.8 to 8.8  
390  $\mu\text{m}$  and continued to increase, with stirring, to a value of 10.5  $\mu\text{m}$ . However, when  
391 vigorous sonication was applied, the new flocs were broken and the particle size  
392 decreased to a value similar to that observed in the curve of PCC. When  
393 sonication was stopped (while maintaining mechanical stirring), the particle size  
394 increased sharply to a  $d_{50}$  value close to 30  $\mu\text{m}$  (more than 3 times the value  
395 observed in the curve of PCC), indicating a high degree of PCC re-flocculation.  
396 For the more carboxylated nanofibrils (CNF11) quite different results were  
397 obtained. Firstly, just after the addition of CNF11 to the PCC suspension, the  
398 increase of the median was very small (from 4.8 to 5.6  $\mu\text{m}$ ) and its value remained  
399 practically constant with time. The subsequent sonication promoted a decrease of  
400 the particle size and, even after stopping it, and with additional mechanical  
401 stirring, the evolution until the end of the experiment was not significant (not  
402 more than 0.2  $\mu\text{m}$ ), the  $d_{50}$  values being even smaller than those obtained for the  
403 experiment with PCC alone.

404

405

Insert Fig. 3

406

407 These results clearly indicate the disability of CNF11 in promoting both PCC  
408 flocculation and re-flocculation, probably because these nanofibrils were adsorbed  
409 at the PCC particles surface by interactions with the  $\text{Ca}^{2+}$  ions and imparted an  
410 excess of negative charge creating high repulsion between particles. On the  
411 contrary, for CNF5, the PCC particles could aggregate much easier (thus

412 contributing to high filler retention in papermaking, Table 2). Patching was most  
413 certainly the dominant mechanism behind flocculation, due to the very small  
414 chain length of the CNF (compared to commonly used flocculants) which  
415 prevented bridging. Besides, according to Korhonen and Laine (2014), only patch  
416 flocculants show reversible flocculation behavior.

417

### 418 **Influence of CNF in the mechanical and structural properties of** 419 **handsheets produced with PCC**

420 Handsheets containing PCC and the aforementioned additives were produced  
421 without CNF and with the two different CNF (CNF5 and CNF11). For  
422 comparison, handsheets without PCC (and containing all the other additives) were  
423 also produced. The values of the corresponding mechanical properties (tensile  
424 index) and of the filler retention are listed in Table 2.

425

426

Insert Table 2

427

428 It is widely reported that the addition of small amounts of CNF to handsheets  
429 composed only of fibres highly increases the tensile index (Saito and Isogai 2007;  
430 González et al. 2012, 2014; Brodin et al. 2014). However, in the presence of the  
431 other additives used in papermaking (including fillers) the influence of the  
432 cellulose nanofibrils on the tensile strength seems not to be as straightforward (Hii  
433 et al. 2012; Ämmälä et al. 2013).

434 The results of the present study confirm that when the handsheets were  
435 produced with all the components except PCC (0% PCC, Table 2) the CNF acted  
436 indeed as a reinforcing material if a moderate TEMPO-mediated oxidation  
437 (CNF5, carboxyl's content 0.63 mmol/g and carboxyl's surface density 3.5  
438 mmol/m<sup>2</sup>) was used: tensile index improvement from 48.1 (±2.6) to 54.9 (±2.8)  
439 N.m/g. On the contrary, if the CNF carboxyl's surface density was high (CNF11,  
440 5.1 mmol/ m<sup>2</sup>), the handsheets tensile index was not significantly different from  
441 that obtained without CNF - a slight trend to decrease from 48.1 (±2.6) to 45.7  
442 (±2.7) N.m/g was even detected. One possible explanation is that the ability of the  
443 CNF to bind with the fibres was now affected by electrostatic interactions  
444 between CNF11 and the positively charged linear CPAM. Besides, some  
445 repulsion between the highly negatively charged CNF and the fibres may have

446 also contributed to increase the inter-fibre distance and therefore decrease the  
447 fibre-to-fibre bonding. Thus, the tensile strength was similar or even worse than  
448 that obtained without CNF. When a lower surface charged CNF was used (CNF5),  
449 these detrimental phenomena were not significant and the potential of the CNF to  
450 enhance the fibre bonding dominated. Hence, as would be expected, an increment  
451 of the tensile strength was observed with CNF5. Furthermore, the smaller degree  
452 of polymerization of CNF11 may have also affected its reinforcing ability  
453 (Kekäläinen et al. 2014; Kobayashi et al. 2016).

454 When mineral fillers were added, the handsheets tensile resistance decreased  
455 significantly, as expected, due to the interference of the filler particles in the fibre-  
456 to-fibre bonding. However, with CNF5, the filler retention was clearly improved  
457 from 89.6 to 93.4% due to its positive role on PCC flocculation (Fig. 3), and even  
458 though the decrease of the tensile strength was not significant (from  $25.0 \pm 0.9$  to  
459  $23.6 \pm 1.0$  N.m/g). This reveals that CNF5 can increase the filler retention without  
460 much disturbing the handsheets mechanical strength.

461 On the other side, for the CNF with a higher carboxyl groups content (CNF11)  
462 the filler retention was highly reduced (from 89.6% without CNF to 66.7%), as a  
463 result of the abovementioned particles repulsion effect that led to a decrease of the  
464 PCC flocculation (Fig. 3), and consequent loss through the wire. Also, some loss  
465 of the nanofibrils during formation is not to be discarded, being this effect more  
466 pronounced for CNF11, with smaller DP. In accordance with the smaller filler  
467 content in the handsheet, the tensile index increased. However, this tensile  
468 increase was expected to be of higher magnitude considering the effective filler  
469 content reduction detected (Lourenço et al. 2014). This did not happen since, as  
470 stated above, on the one hand, CNF11 limit the fibre-to-fibre bonding and on the  
471 other hand the cationic polyacrylamide is preferentially linked to CNF11. As a  
472 result, it is not so available for filler retention and bridging effects, besides  
473 creating CNF-CPAM bundles that do not allow fibres to bind so effectively.

474 Fig. 4 attempts to explain the mechanisms behind the interactions between the  
475 fibres, the positively charged filler particles, the negatively charged CNF samples  
476 and the linear cationic polyacrylamide considering the results presented so far.  
477 When CNF5 is added to the PCC suspension, larger flocs are formed, being  
478 patching the dominant mechanism, with the nanofibrils adsorbed at the particles  
479 surface, as described above. Next, the linear cationic polyacrylamide promotes

480 bonds between flocs and also between flocs and fibres, by the bridging  
481 mechanism. Some bridging effect of the CNF5 nanofibrils with the fibres is not  
482 also to be discarded (Korhonen and Laine 2014). Covalent linkages between  
483 CPAM and CNF are reported in the literature (Saito and Isogai 2007). These  
484 phenomena explain the aforementioned impact of CNF5 both on filler retention  
485 and on tensile strength. The opposite occurs with CNF11 (which has more than  
486 the double of carboxylic groups) due to the referred to repulsion effects and to the  
487 formation of bundles with CPAM. Moreover, the eventual bridging between these  
488 nanofibrils and the fibres is less likely to occur with the same extent, due to their  
489 smaller DP/length.

490

491

Insert Fig. 4

492

493 FE-SEM images of the handsheets without CNF and also with CNF5 are depicted  
494 in Fig.5 for two magnifications. At  $2k \times$  magnification filler aggregates at the  
495 fibres surface and between fibres are visible for both structures. Higher resolution  
496 images ( $20k \times$ ) in the areas where the precipitated calcium carbonate particles are,  
497 show a much more complex matrix when the CNF5 are used. The nanofibrils  
498 network is now visible and it is clearly evident its flocculating and binding effect.

499

500

Insert new Fig. 5

501

502 Due to the undesirable results observed with CNF11, the influence on the wet-  
503 web resistance of handsheets produced with different moisture contents was  
504 assessed only with CNF5. The results are depicted in Fig. 6. As can be seen, the  
505 CNF impact CNF on the handsheets tensile resistance was remarkable, especially  
506 for moisture contents below 60% - gains of up to 100% can be noticed. For  
507 moisture contents superior to 60% this impact was not so evident, although still  
508 positive. ~~as visible in the right plot of Fig. 6.~~ For these conditions of excess of  
509 water, the chemical interactions were expectedly weak. Remarkably, the influence  
510 of CNF was more pronounced for the wet-strength (of handsheets with water  
511 content up to 60%) than for the dry strength. Similar conclusions were reported by  
512 Saito and Isogai (2007), but in systems without mineral fillers. No studies of the  
513 CNF influence on the wet-web strength are available in the open literature for

514 filler-containing papers. These results are of utmost importance for the runnability  
515 of the paper machine: for moisture contents common in the drying section (7-  
516 50%), CNF may contribute, through the higher wet-web tensile resistance, to  
517 reduce break events and/or to increase operating machine speeds.

518

519 Insert new Fig. 6

520

521

522 Besides the mechanical resistance analysis, the drainability of the handsheets  
523 production process (evaluated by measuring the drainage time) and the structural  
524 properties of the dried handsheets were also examined. The results are presented  
525 in Table 3.

526 Regarding the use of CNF5, the drainage time was negatively affected (a  
527 relative increase of *ca.* 70% was detected), as a consequence of its hydrophilic  
528 character and its role on densifying the fibrous matrix, in agreement with the  
529 mechanisms described before. After drying, handsheets with less empty spaces  
530 than those produced without CNF are obtained, having a more compact 3D-  
531 structure. Accordingly, the air resistance increased significantly and the bulk  
532 decreased when CNF5 was used.

533 On the other side, the loss of filler detected when CNF11 was used (Table 2)  
534 was clearly confirmed by the decrease of the handsheets basis weight. The smaller  
535 filler content contributed to a higher fibre-to-fibre available bonding area, when  
536 comparing with the handsheets produced with 30% of PCC, and led, as expected,  
537 to an increase of the drainage time and of the air resistance. Even though, this  
538 increase was limited due to the abovementioned effect of CNF11 on preventing  
539 fibre-to-fibre bonding. From the smaller basis weight a higher value of bulk  
540 would be expected but this effect was balanced by the small amount of material  
541 (resulting from the filler loss) and the subsequent reduction of the handsheets  
542 thickness (114 $\mu$ m vs. 133 $\mu$ m).

543

544 Insert Table 3

545

546 Finally, the porosity of the handsheets produced with the CNF samples was  
547 evaluated by mercury intrusion porosimetry (Fig.7). The results of the total



548 porosity of the handsheets are in close agreement with those of the air resistance,  
549 the handsheets with CNF11 presenting intermediate values (and having also a  
550 higher percentage of larger pores).

551

552

Insert Fig. 7

553

554 One of the goals in the papermaking industry is to be able to use higher  
555 amounts of filler in paper without disturbing other properties like the mechanical  
556 strength and bulk. The results of this study revealed that by adding to a paper  
557 furnish (containing fibres, PCC, starch and a cationic polyacrylamide) 3 wt% of  
558 TEMPO oxidized CNF (containing 0.6 mmol carboxyl groups per g of pulp), it is  
559 possible to slightly increase the filler content without affecting the mechanical  
560 strength of the dry handsheets, and also to increase very significantly the tensile  
561 strength of handsheets with moisture contents up to 60 %. It was shown that this  
562 does not occur when the chemical pre-treatment is harsher, leading to high surface  
563 charged cellulose nanofibrils with small length. In spite of the aforementioned  
564 improvements, the handsheets freeness is hindered, being therefore advisable for  
565 future work to test other drainage aids. Overall, the main advance of this work is  
566 the study of the influence of different TEMPO-oxidized CNF in the papermaking  
567 properties when all the furnish components are considered, concluding that they  
568 may act as strength reinforcing agents (in the wet end section) and as flocculants  
569 if a mild TEMPO-mediated oxidation is used for their production.

570

571

## 572 **Conclusions**

573 In this work, the influence in papermaking of cellulose nanofibrils produced  
574 by TEMPO-mediated oxidation and possessing different contents of carboxyl  
575 groups and degree of polymerization has been evaluated. It was found that a CNF  
576 having 0.6 mmol/g of carboxyl groups and a yield of nanofibrillated material  
577 around 90 wt% (CNF5) was much more favorable for the PCC (filler) retention in  
578 the paper matrix than a slightly more fibrillated (97 wt% yield) but also more  
579 charged and smaller in length CNF (CNF11, with 1.5 mmol/g of carboxyl groups  
580 and a DP of 203). In fact, for furnish compositions similar to those used in  
581 papermaking (eucalyptus fibres, PCC, internal sizing agent, starch, and retention

582 aid), the addition of 3 wt% of CNF5 increased the filler retention relatively to that  
583 obtained without nanofibrillar material, whereas the addition of CNF11 had an  
584 opposite effect. Flocculation studies carried out by laser diffraction spectrometry  
585 showed that CNF5 promoted the formation of large size flocs (with a median  
586 diameter of the particle size distribution up to almost 30  $\mu\text{m}$ ), which are  
587 considered to be responsible for the high filler retention. On the other hand, with  
588 CNF11, the median diameter of the PCC flocs was not larger than 5.5  $\mu\text{m}$ ,  
589 revealing that these more charged nanofibrils did not act as flocculant and by the  
590 contrary, caused some repulsion between particles. The influence of the CNF on  
591 the drainability and on some papermaking properties such as tensile strength and  
592 air permeability was also assessed for handsheets both without and with fillers,  
593 and the results were interpreted in terms of the reinforcing potential of the  
594 nanofibrillar material – this potential varied mainly as a function of the CNF  
595 carboxyl groups content, being also affected by their length, in such a way that the  
596 more charged and smaller CNF (1.5 mmol/g and DP of 203) exhibited a negative  
597 role on fibre bonding. A mechanism to explain the interactions between the fibres,  
598 CNF, fillers and a cationic polyelectrolyte retention agent (CPAM) was proposed.

599 Another important finding of this work was related to the ability of CNF5 in  
600 improving the wet-web resistance of the *E. globulus* bleached kraft pulp based  
601 handsheets with a nominal filler content close to 30% and in a wide range of  
602 moisture contents (between 10 and 70%). The well-known capability of the CNF  
603 to increase the tensile strength of cellulose matrices without minerals was now  
604 also confirmed for filler-containing papers even at high moisture contents. When  
605 CNF5 was used the tensile strength greatly increased to almost the double of the  
606 values obtained without CNF, even at moisture contents above 50%.

607 Overall, this study confirms that TEMPO-oxidized CNF may be used in  
608 papermaking simultaneously as reinforcing agent and flocculant, despite the  
609 complex interactions between all the paper furnish components. Nonetheless, their  
610 influence is much dependent on their structure, namely charge, but also size, as  
611 proved in this work.

612

## 613 **Acknowledgments**

614 The authors acknowledge PhD Ricardo Serra from the Department of Mechanical Engineering of  
615 the University of Coimbra for his valuable cooperation in the AFM analysis.

616 Ana F. Lourenço would like to acknowledge Fundação para a Ciência e Tecnologia (FCT),  
617 Portugal, for PhD grant SFRH/BDE/108095/2015.  
618

## 619 **References**

- 620 Ämmälä A, Liimatainen H, Burmeister C, Niinimäki J (2013) Effect of tempo and periodate-  
621 chlorite oxidized nanofibrils on ground calcium carbonate flocculation and retention in sheet  
622 forming and on the physical properties of sheets. *Cellulose* 20: 2451-2460
- 623 Besbes I, Alila S, Boufi S (2011) Nanofibrillated cellulose from TEMPO-oxidized eucalyptus  
624 fibres: Effect of the carboxyl content. *Carbohydrate Polymers* 84: 975-983
- 625 Brodin FW; Gregersen OW; Syverud K (2014) Cellulose nanofibrils: challenges and possibilities  
626 as a paper additive or coating material – a review. *Nord Pulp Paper Res J* 29: 156-166
- 627 Chinga-Carrasco G, Tobjörk D, Österbacka R (2012) Inkjet-printed silver-nanoparticles on nano-  
628 engineered cellulose films for electrically conducting structures and organic transistors –  
629 concept and challenges. *J Nanopart Res* 14: 1213
- 630 Eichorn S, Dufresne A, Aranguren M, Marcovich N E, Capadona J R, Rowan S J, Weder C,  
631 Thielemans W, Roman M, Renneckar S, Gindl W, Veigel S, Keckes J, Yano H, Abe K, Nogi  
632 M, Nakagaito A N, Mangalam A, Simonsen J, Benight A S, Bismarck A, Berglund L A, Peijs  
633 T (2010) Review: current international research into cellulose nanofibres and nanocomposites.  
634 *J Mater Sci* 45: 1-33
- 635 Espinosa E, Tarrés Q, Delgado-Aguilar M, González I, Mutjé P, Rodríguez A. (2016) Suitability  
636 of wheat straw mechanical pulp for the fabrication of lignocellulosic nanofibres and their  
637 application to papermaking slurries. *Cellulose* 23:837-852
- 638 Fukuzumi H, Saito T, Iwata T, Kumamoto Y, Isogai A (2009) Transparent and highgas barrier  
639 films of cellulose nanofibers prepared by TEMPO-mediated oxidation. *Biomacromolecules*  
640 10: 162-165
- 641 Gamelas JAF, Pedrosa J, Lourenço AF, Mutjé P, Chinga-Carrasco G, Singh G, Ferreira PJT  
642 (2015a) On the morphology of cellulose nanofibrils obtained by TEMPO-mediated oxidation  
643 and mechanical treatment. *Micron*: 72: 28-33
- 644 Gamelas JAF, Pedrosa J, Lourenço AF, Ferreira PJ (2015b) Surface properties of distinct  
645 nanofibrillated celluloses assessed by inverse gas chromatography. *Colloids Surf. A* 469: 36-  
646 41
- 647 González I: Boufi S, Pèlach M, Alcalà M, Vilaseca F, Mutjé P (2012) Nanofibrillated cellulose as  
648 a paper additive in eucalyptus pulps. *BioResources* 7(4): 5167-5180
- 649 González I, Alcalà M, Chinga-Carrasco G, Vilaseca F, Boufi S, Mutjé P (2014) From paper to  
650 nanopaper: evolution of mechanical and physical properties. *Cellulose* 21: 2599–2609
- 651 Hänninen T, Orelma H, Laine J (2015) TEMPO oxidized cellulose thin films analysed by QCM-D  
652 and AFM. *Cellulose* 22: 165-171
- 653 He M, Cho B-U, Won J M (2016) Effect of precipitated calcium carbonate - Cellulose nanofibrils  
654 composite filler on paper properties. *Carbohydrate Polymers* 136: 820–825
- 655 Henriksson M, Berglund L, Isaksson P, Lindström T, Nishino T (2008) Cellulose Nanopaper  
656 Structures of High Toughness. *Biomacromolecules* 9: 1579–1585
- 657 Hii C, Gregersen Ø W, Chinga-Carrasco G, Eriksen Ø (2012) The effect of MFC on the  
658 pressability and paper properties of TMP and GCC based sheets. *Nordic Pulp and Paper*  
659 *Research Journal* 27(2): 388-396
- 660 Hubbe MA (2014) Prospects for maintaining strength of paper and paperboard products while  
661 using less forest resources: a review. *BioResources* 9(1): 1634-1763
- 662 Ioelovich M, Figovsky O (2010) Structure and properties of nanoparticles used in paper  
663 compositions. *Mechanics of Composite Materials* 46(4): 435-442
- 664 Isogai A, Saito T, Fukuzumi H (2011) TEMPO-oxidized cellulose nanofibers. *Nanoscale* 3: 71-85
- 665 Kangas H, Lahtinen P, Sneek A, Saariaho A-M, Laitinen O, Hellén E (2014) Characterization of  
666 fibrillated celluloses A short review and evaluation of characteristics with a combination of  
667 methods. *Nordic Pulp Pap Res J* 29(1): 129-143
- 668 Kekäläinen K, Liimatainen H, Illikainen M, Maloney TC, Niinimäki J (2014). The role of the  
669 hornification in the disintegration behaviour of TEMPO-oxidized bleached hardwood fibres in  
670 a high-shear homogenizer. *Cellulose* 21: 1163-1174
- 671 Khalil H, Davoudpour Y, Islam M, Mustapha A, Sudesh K, Dungani R, Jawaid M (2014)  
672 Production and modification of nanofibrillated cellulose using various mechanical processes:  
673 A review. *Carbohydrate Polymers* 99: 649- 665

674 Klemm D, Kramer F, Moritz S, Lindström T, Ankerfors M, Gray D, Dorris A (2011)  
675 Nanocelluloses: A New Family of Nature-Based Materials. *Angew Chem Int Ed* 50: 5438 –  
676 5466

677 Kobayashi Y, Gondo T, Yamamoto M, Saito T, Isogai A (2016) Fundamental properties of  
678 handsheets containing TEMPO-oxidized pulp in various weight ratios. *Nordic Pulp Paper*  
679 *Research Journal* 31(2): 248-254

680 Korhonen M H J, Laine J (2014) Flocculation and retention of fillers with nanocelluloses. *Nordic*  
681 *Pulp Paper Research Journal* 29(1): 119-128

682 Lavoine N, Desloges I, Dufresne A, Bras J (2012) Microfibrillated cellulose – its barrier properties  
683 and applications in cellulosic materials: a review. *CarbohydrPolym* 90: 735-764

684 Lourenço AF, Gamelas JA, Ferreira PJ (2014) Increase of the filler content in papermaking by  
685 using a silica-coated PCC filler. *Nordic Pulp Pap Res J* 29: 240-245

686 Petroudy SRD, Syverud K, Chinga-Carrasco G, Ghasemain A, Resalati H (2014) Effects of  
687 bagasse microfibrillated cellulose and cationic polyacrylamide on key properties of bagasse  
688 paper. *Carbohydrate Polymers* 99: 311-318

689 Rasteiro, MG, Garcia, FAP, Ferreira P, Blanco A, Negro C, Antunes E (2008) Evaluation of flocks  
690 resistance and reflocculation capacity using the LDS technique. *Powder Technology* 183 231-  
691 238.

692 Raymond L, Turcotte R, Gratton R (2004) The challenges of increasing filler in fine paper. *Paper*  
693 *Technology* 45(6): 34-40

694 Saito T, Isogai A (2004) TEMPO-Mediated Oxidation of Native Cellulose The Effect of Oxidation  
695 Conditions on Chemical and Crystal Structures of the Water-Insoluble Fractions.  
696 *Biomacromolecules* 5: 1983-1989

697 Saito T, Isogai A (2006) Introduction of aldehyde groups on surfaces of native cellulose fibers by  
698 TEMPO-mediated oxidation. *Colloids Surf A: Physicochem Eng Aspects* 289: 219-225

699 Saito T, Isogai A (2007) Wet strength improvement of TEMPO-oxidized cellulose sheets prepared  
700 with cationic polymers. *Ind Eng Chem Res* 46: 773-780

701 Saito T, Kimura S, Nishiyama Y, Isogai A (2007) Cellulose nanofibres prepared by TEMPO-  
702 mediated oxidation of native cellulose. *Biomacromolecules* 8: 2485-2491

703 Saito T, Hirota M, Tamura N, Kimura S, Fukuzumi H, Heux L, Isogai A. (2009) Individualization  
704 of Nano-Sized Plant Cellulose Fibrils by Direct Surface Carboxylation Using TEMPO  
705 Catalyst under Neutral Conditions. *Biomacromolecules* 10: 1992-1996

706 Saraiva MS, Gamelas JAF, de Sousa APM, Reis BM, Amaral JL, Ferreira PJ (2010) A New  
707 Approach for the Modification of Paper Surface Properties Using Polyoxometalates. *Materials*  
708 3: 201-215

709 Syverud K, Stenius P (2009) Strength and barrier properties of MFC films. *Cellulose* 16: 75–85

710 Taipale T, Österberg M, Nykänen A, Ruokolainen J, Laine J (2010) Effect of microfibrillated  
711 cellulose and fines on the drainage of kraft pulp suspension and paper strength. *Cellulose* 17:  
712 1005-1020

713 Torvinen K, Sievänen J, Hjelt T, Hellén E (2012) Smooth and flexible filler- nanocellulose  
714 composite structure for printed electronics applications. *Cellulose* 19: 821-829  
715

716 **Table 1.** CNF characterization data.

Sample	Yield (%)	CD <sup>a</sup> (μeq g/g)	C <sub>COOH</sub> <sup>b</sup> (mmol/g)	DP <sup>c</sup>	DS <sup>d</sup>	SSA <sup>e</sup> (m <sup>2</sup> /g)	Diameter (nm)	Z Average - DLS
CNF5	91	997	0.63	548	0.10	181	14.7	2327
CNF11	97	2188	1.56	203	0.27	307	8.7	323

717 <sup>a</sup> Cationic Demand; <sup>b</sup> Carboxyl group's content; <sup>c</sup> Degree of polymerization; <sup>d</sup> Specific Surface  
718 Area.

719 **Table 2.** Tensile index of handsheets produced with CNF and PCC and also of the reference  
 720 (without CNF or without PCC) \*.

CNF	0% PCC	30 % PCC	
	Tensile Index, N.m/g	Tensile Index, N.m/g	Filler Retention, %
0	48.1 (2.6)	25.0 (0.9)	89.6 (0.1)
3% CNF5	54.9 (2.8)	23.6 (1.0)	93.4 (0.7)
3% CNF11	45.7 (2.7)	28.5 (1.5)	66.7 (0.3)

721 \*all the handsheets contained CPAM, starch and ASA; in parenthesis the standard deviation.  
 722

723 **Table 3** Properties of the handsheets produced with and without CNF. \*

Sample	Drainage time, s	Basis weight, g/m <sup>2</sup>	Bulk, cm <sup>3</sup> /g	Air Resistance (Gurley), s/100 ml
30% PCC – 0% CNF	5.6 (0.1)	80.1 (0.3)	1.66 (0.01)	3.3 (0.2)
30% PCC – 3% CNF5	9.5 (0.5)	83.5 (0.4)	1.58 (0.03)	12.8 (1.4)
30% PCC – 3% CNF11	6.2 (0.2)	72.0 (0.8)	1.58 (0.04)	5.2 (0.6)

\* in parenthesis the pooled standard deviation of two series of measurements

724

725

726

727 **Figure captions**

728

729 **Fig 1** FTIR-ATR spectra of films of CNF5 and CNF11 highlighting the  
730 asymmetric COO stretching band.

731 **Fig. 2** Nanofibrils diameter distribution obtained by AFM for both samples (a)  
732 and AFM image in phase imaging mode of sample CNF5 (b).

733 **Fig. 3** Influence of the addition of CNF5 and CNF11 in the median ( $d_{50}$ ) of the  
734 particle size distribution of PCC flocs measured by laser diffraction spectrometry.  
735 An experiment carried out with only PCC is also presented for comparison.

736 **Fig. 4** Schematic representation of the bonding mechanism between PCC, CNF,  
737 fibres and retention agent (CPAM). The left side of the scheme corresponds to  
738 CNF5 and the right side to CNF11.

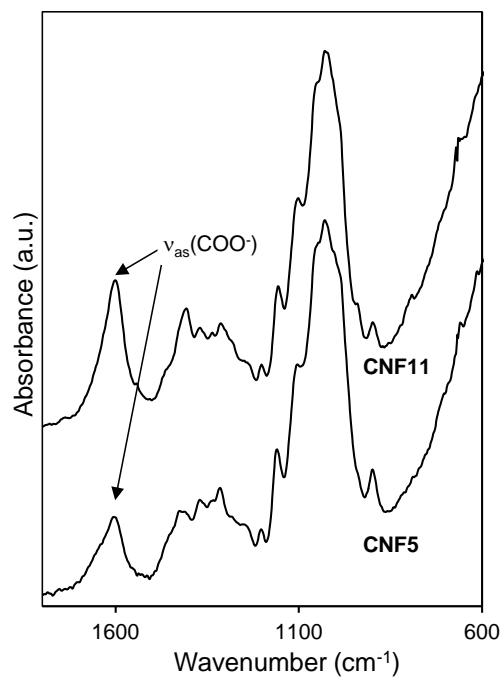
739 **Fig. 5** FE-SEM images of handsheets produced without CNF5 (a,c) and with  
740 CNF5 (b,d). The narrow arrows indicate the PCC particles and agglomerates and  
741 the thicker arrows the CNF network.

742 **Fig. 6** Tensile resistance of handsheets produced with CNF5 (square) and without  
743 CNF (cross) for different moisture contents.

744 **Fig. 7** Hg intrusion porosity of handsheets produced with PCC (a) and with PCC  
745 and CNF5 (b) or CNF11 (c).

746



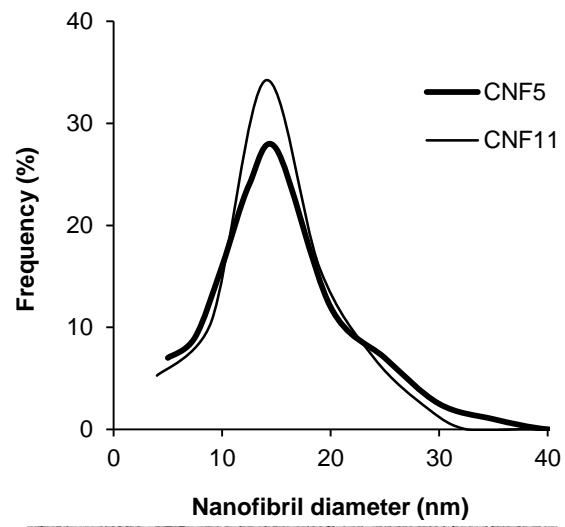


747

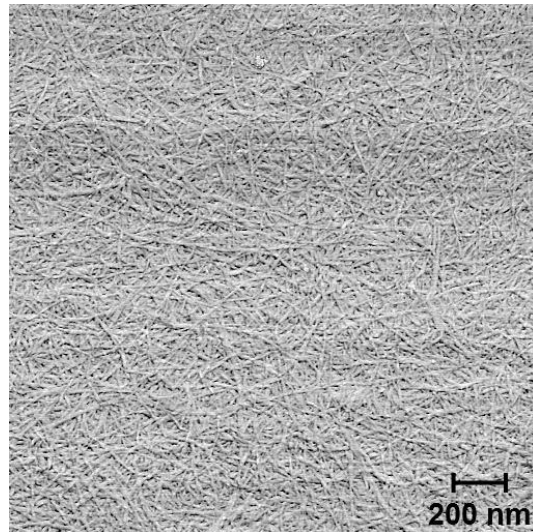
748 **Fig 1** FTIR-ATR spectra of films of CNF5 and CNF11 highlighting the asymmetric COO  
749 stretching band.

750

751



752



753

754

(a)

(b)

755

756

**Fig. 2** Nanofibrils diameter distribution obtained by AFM for both samples (a) and AFM image in phase imaging mode of sample CNF5 (b).

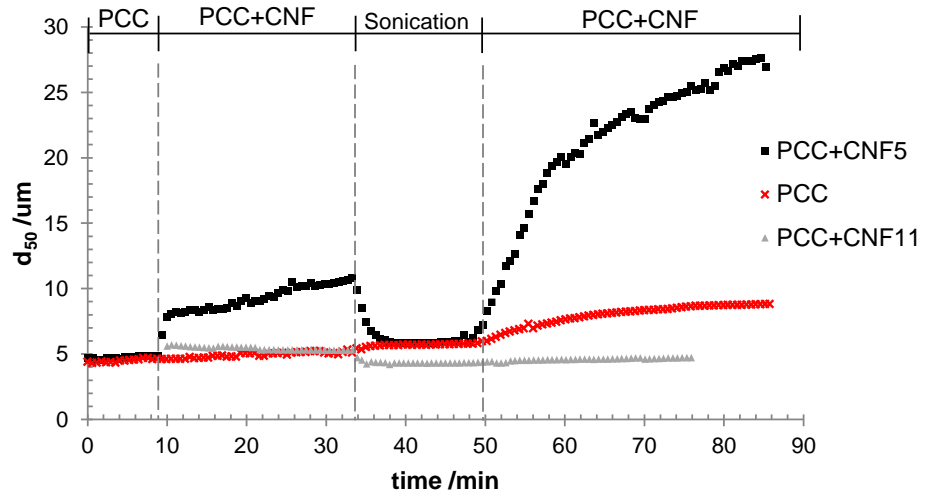
757

758

759

760

761



762

763

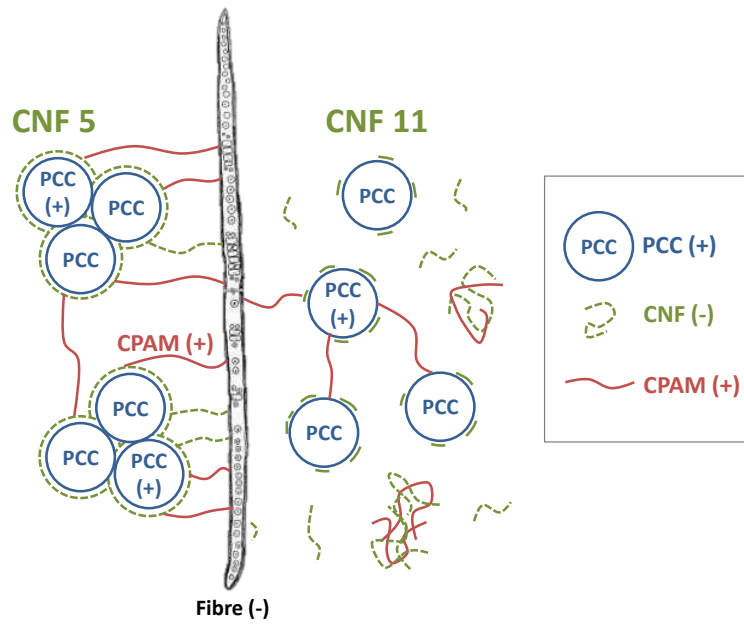
764

765

766

**Fig. 3** Influence of the addition of CNF5 and CNF11 in the median ( $d_{50}$ ) of the particle size distribution of PCC flocs measured by laser diffraction spectrometry. An experiment carried out with only PCC is also presented for comparison.

767



768

769

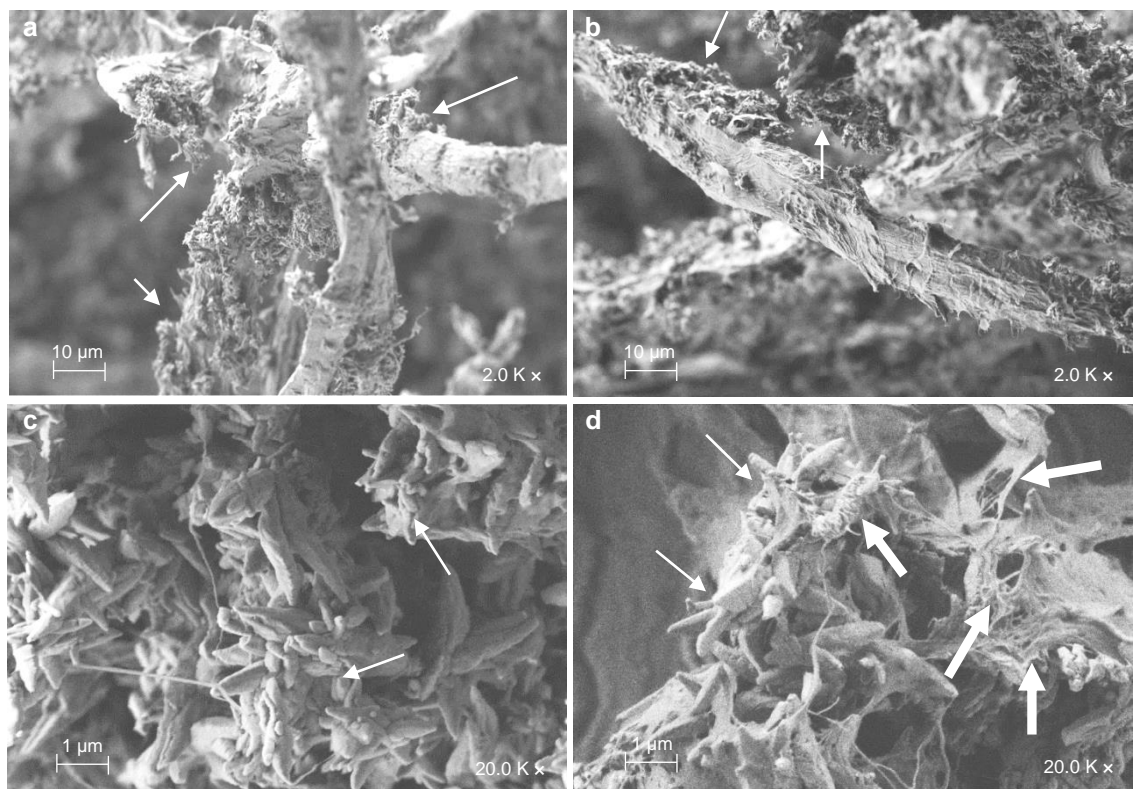
770

771

772

**Fig. 4** Schematic representation of the bonding mechanism between PCC, CNF, fibres and retention agent (CPAM). The left side of the scheme corresponds to CNF5 and the right side to CNF11.

773



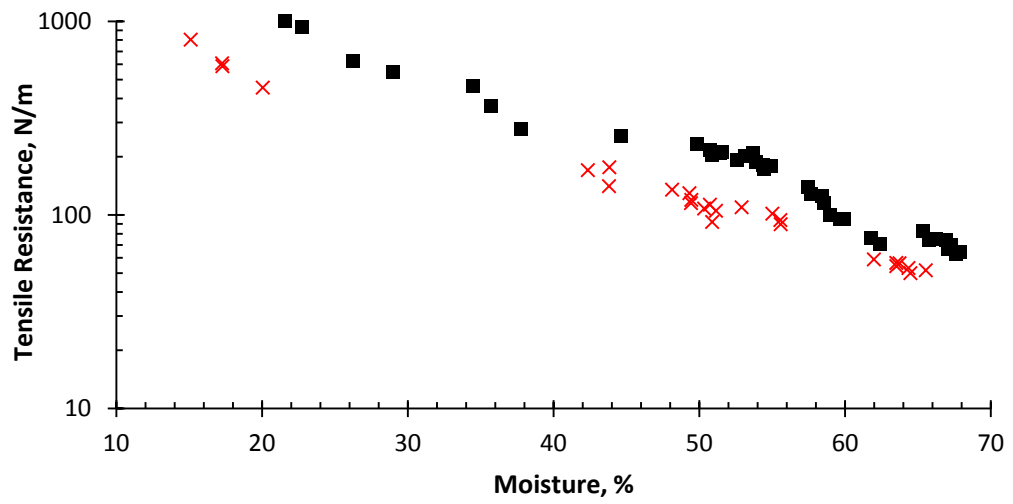
774

775 **Fig. 5** FE-SEM images of handsheets produced without CNF5 (a,c) and with CNF5 (b,d). The  
776 narrow arrows indicate the PCC particles and agglomerates and the thicker arrows the CNF  
777 network.

778

779

780



781

782

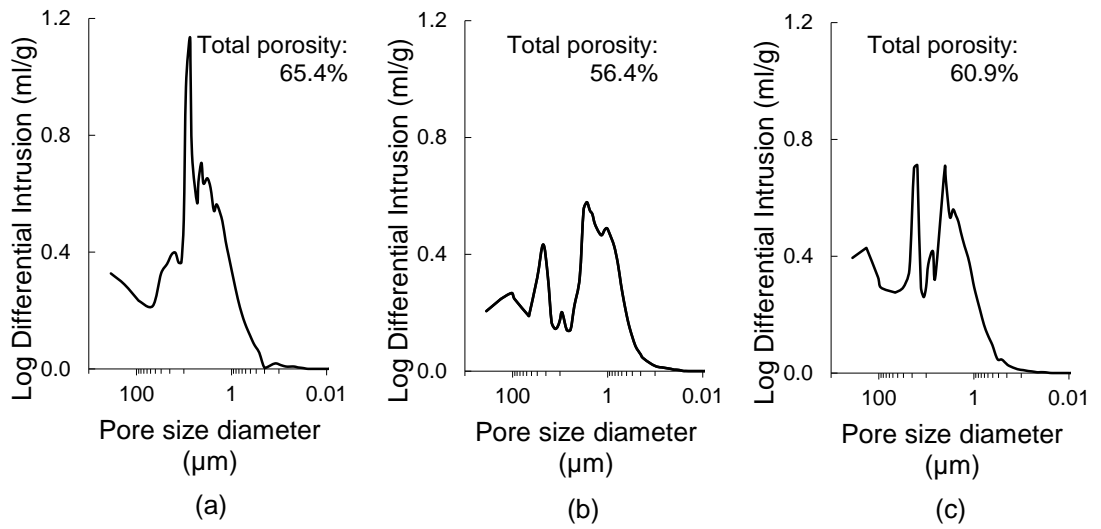
783

**Fig. 6** Tensile resistance of handsheets produced with CNF5 (square) and without CNF (cross) for different moisture contents.

784

785

786



787

788

789

790

**Fig. 7** Hg intrusion porosity of handsheets produced with PCC (a) and with PCC and CNF5 (b) or CNF11 (c).

791

792